NANOSYSTEMS: PHYSICS, CHEMISTRY, MATHEMATICS, 2013, 4 (2), P. 206–213

SPATIAL-TIME PATTERN OF ELECTRICAL FIELD OF TERAHERTZ PULSE IN THE FAR FIELD

M. S. Kulya[1], Ya. V. Grachev[1], V. G. Bespalov[1], V. P. Kujanpaa[2]

[1]St. Petersburg National Research University of Information Technologies, Mechanics and Optics, Saint Petersburg, Russia
[2]VTT Technical Research Centre of Finland, Finland

maxk2350@yandex.ru, grachev_y@mail.ru, victorbespaloff@gmail.com, veli.kujanpaa@vtt.fi

The spatial and temporal dependence of the electric field amplitude of a terahertz (THz) pulse of several oscillations in the far field near the focal plane of a parabolic mirror was experimentally obtained. During experimentation a space-time anomaly was discovered in the diffraction patterns. In the wave front of the field the amplitude decreases to zero, and going through this spatial plane, the phase of oscillations changes, while in the integrated intensity, there is a dip in the curve. The results can be applied in pulsed terahertz optics and spectroscopy.

Keywords: THz electric field pulsed THz radiation, diffraction, pulses of a few electromagnetic field oscillation.

1. Introduction

Terahertz (THz) radiation lies in the frequency range 0.1–10 THz, which corresponds to wavelengths between the infrared and millimeter/submillimeter range from 0.03–3 mm. The physics and technology of THz radiation is not new [1], however, the development of femtosecond optics and microelectronics has permitted significant progress in this field. Correspondingly, interest in basic and applied research has increased, and recent monographs have been published [2, 3]. Methods for obtaining and detecting THz radiation were established using femtosecond pulses of light when excited charge carriers of semiconductors and superconductors [2–5], with optical detection in $\chi(2)$ nonlinear media [6], in optical breakdown of gases and radiation of first and second harmonic of a femtosecond laser [7, 8] .

One of the fundamental phenomena of optics is the diffraction of light, but experimental studies of the spatial and temporal structure of ultra short broadband pulses, which have a complex amplitude-phase structure, have not been sufficiently carried out [9–12]. Experimentally, it is difficult to study the diffraction of a few electromagnetic field oscillation pulses for the wavelengths of visible and infrared ranges of the spectrum. This is because there is practically no possibility for the direct detection of the amplitude and phase, and only iterative calculation procedures can be used to recover the original temporal or spatial profile [13].

The experimental study of the diffraction of an ultra short pulse with a complex amplitude-phase structure became possible only with the advent of methods for recording temporal forms of an electric field pulse of broadband THz radiation. The THz wave front usually has only a few oscillations of the electromagnetic field. The wave front also has a complex amplitude-phase structure, which is connected with the process of its generation, further diffraction on the formed aperture, and with the influence of the medium's dispersion [14, 15].

The aim of this work was to obtain the spectral and temporal shape of the electric field of a THz pulse from a few oscillations with a broadband spectrum and of picoseconds duration. The particular feature of this research is the direct detection of the spatial-time form of extremely short pulses, which was difficult in the optics of long pulses, as the photodetectors measure only field intensity. This study may be useful in interpreting the results of measurements in pulsed THz optics and spectroscopy.

2. Experimental Setup

The scheme of experimental arrangement is shown in Fig. 1. A femtosecond laser beam *Yb:KYW* laser *FL-1* (wavelength $\lambda p = 1040$ nm, beam diameter $d = 2$ mm, the pulse width at half-width $\tau \geq 120$ fs, repetition rate of 80 MHz, average power $W = 1.2$ W) with use of a beam splitter *BS* is divided into a probe beam and a pump beam. The pump beam passes through an optical delay line (Delay). It falls on a semiconductor crystal *InAs*, placed in a constant magnetic field M, where THz radiation is generated [5]. The plane of the crystal coincides with the focal plane of a parabolic mirror *PM1* with focal length of 90 mm and an optical aperture of 60 mm. THz radiation is collimated by a parabolic mirror *PM1* behind which there is a teflon filter *F*, transmitting THz radiation and scattering powerful femtosecond laser infra-red radiation. In addition, horizontal polarization is separated by a polarizer *P*. After passing along the optical path in the air $L = 25$ cm, THz radiation is focused by a parabolic second mirror *PM2* on the electro-optical crystal *CdTe*, with an area of 10×10 mm^2 and a thickness of 2 mm. This crystal is most suitable for electro-optic detection of THz radiation due to its dispersion properties [16, 17].

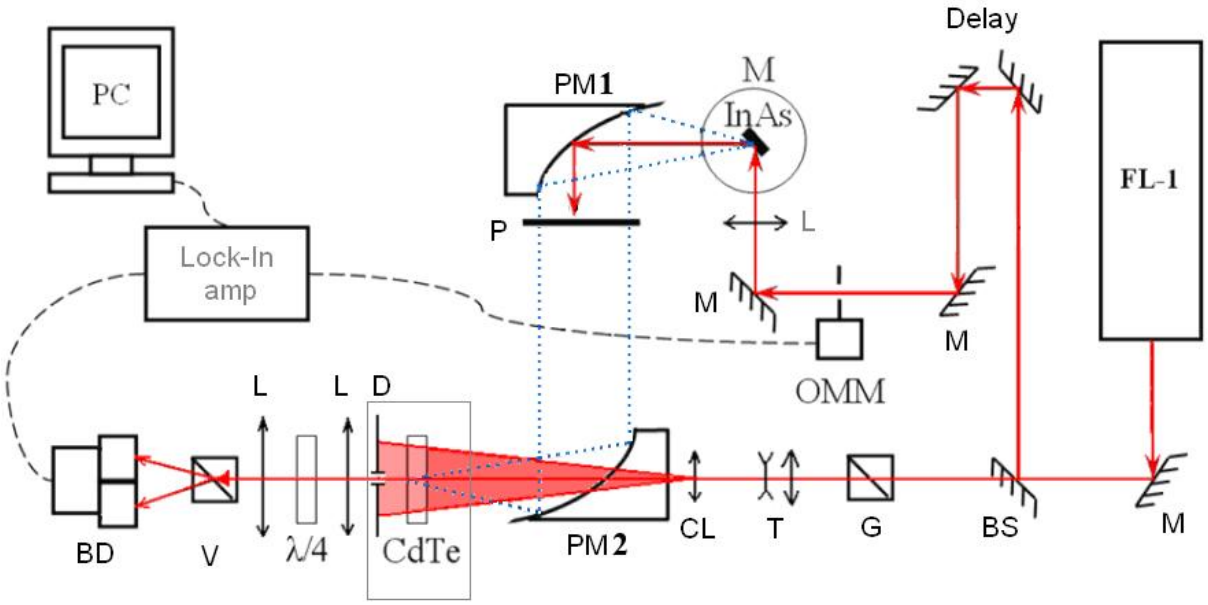

FIG. 1. The experimental scheme: *Yb: KYW* laser *FL-1* ($\lambda = 1040$ nm, $\tau \approx 200$ fs, repetition rate of 80 MHz, $W = 1.2$ W); *BS* —beam splitter; *G* — Glan prism; *M* —magnet; *CL* —cylindrical lens; *T* —telescopic system; *D* — diaphragm; *L* — lens; *PM* —parabolic mirror; *OMM* —optical-mechanical modulator; *P* — Teflon filter; *V* — Wollaston prism; *BD* — balanced detector. Solid lines — femtosecond laser infra-red radiation; dot lines — THz radiation

After the femtosecond laser probe beam passes a Glan prism *G*, its radiation obtains horizontal linear polarization with an accuracy of 10^{-4}. Then, the telescope *T* increases the diameter of the beam to about 5 mm, and the cylindrical lens *CL* focuses the radiation on the central region of the crystal *CdTe*. Thus a rectangular shaped spot of the probe radiation is formed on the crystal, the larger being directed dimension towards the horizontal axis x. When the probe beam propagates through the electro-optical crystal *CdTe*, it is influenced by the constant electric field of collinearly propagating THz pulse, which affects the linear polarization of the probe beam and change it to elliptical polarization. A quarter-wave plate $\lambda/4$ transforms

the probe beam polarization to near-circular polarization. The beams with different polarization states are separated by a Wollaston prism *V* and they fall on the balanced detector *BD*. Since the magnitude of the birefringence is directly proportional to the electric field, the intensity difference on the balanced circuit photodiodes is also proportional to the field of THz radiation. The signal from the balanced detector enters the lock-in amplifier, consistent with the optical modulator *OMM* and then the signal goes to an analog-to-digital converter built into the *PC*.

The optical delay line *Delay* changes the crossing time of THz radiation and the probe beam in the crystal. Thus, by measuring the effect of birefringence for various delays, the dependence of the amplitude of the electric field of the terahertz pulse on time $E_{THz}(t)$ can be recorded.

A firmly fixed aperture with a diameter of 1 mm was placed after the crystal *CdTe*, in order to study the spatial and temporal form of the THz pulse, Fig. 2. With movement of the recording system in the horizontal x and vertical y directions the point-to-point detection of the THz field in the focal plane of the cylindrical lens $E_{THz}(x, y, t)$ was provided.

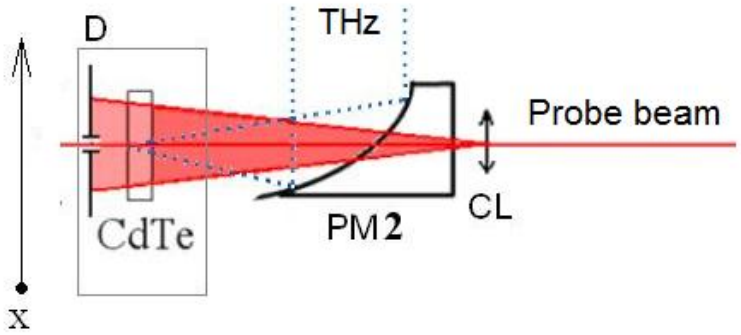

FIG. 2. Scheme of point-to-point measurement of THz field. Solid lines — femtosecond laser infra-red radiation; dot lines — THz radiation

The optical system of two parabolic mirrors (*PM1, PM2*) transfers the image (size d) illuminated by the beam of femtosecond laser on the crystal *InAs* into the plane of the electro-optical crystal *CdTe*. As THz radiation is formed only in the illuminated region [2,3], a far field THz radiation is formed in the focal plane of a parabolic mirror *PM2* (electro-optical detector plane of *CdTe*). The dimensions of the far field THz radiation are defined by the size of the generation region and THz wavelength range. The spectrum covered by the THz generator includes 0.1 – 1.7 THz (wavelengths 3,000–176 μm) [18], with a maximum of intensity at 0.6–0.7 THz ($\lambda \sim 500$ μm $< d$). The maximum size of the diffraction pattern of THz radiation in the plane of the electro-optical detector *CdTe* can be estimated to be equal to d. As the spectrum contains wavelengths larger than d, the size of the area will increase accordingly.

The measurements of the spatial-time pattern of the diffraction were made with different pump beam geometries, illuminating the *InAs* crystal generating the THz radiation. Fig. 3 shows the spatial profiles with different apertures. Fig. 3a describes the pump beam profiles of the femtosecond laser of aperture $d = 2$ mm and Fig. 3b shows a focused laser beam with aperture value $d = 1$ mm. Fig. 3c and d show the rectangular beams created by the introduction of a cylindrical lens in the scheme of the laser beam. It should be noted that by focusing with the cylindrical lens, the generated area on the x-coordinate is a sub-wavelength for THz radiation, which affects the distribution of the far field.

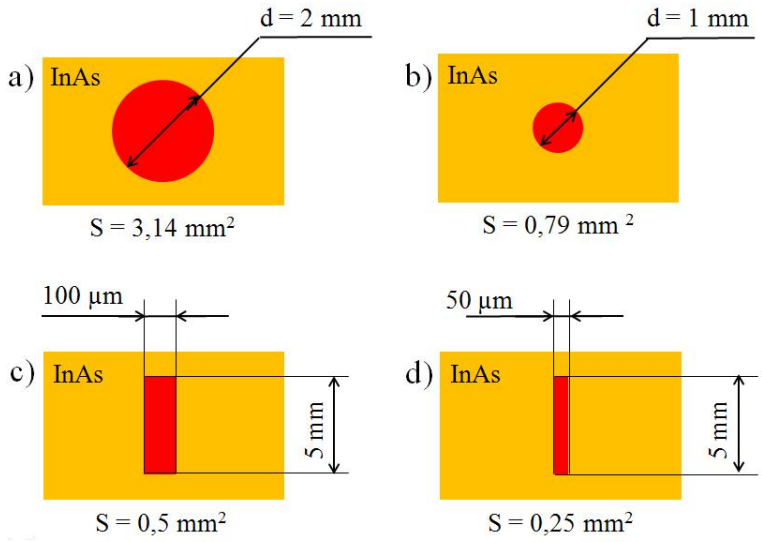

FIG. 3. Spatial profile of the pump beam incident on the crystal *InAs* generating THz radiation: a femtosecond laser source aperture $d = 2$ mm (a), a focused laser beam diameter of 1 mm (b), beams of quasi-rectangular forms created by the introduction of a cylindrical lens in the scheme of the laser beam (c, d)

3. Experimental Results

By moving the mobile measurement system, Fig. 2, the point where the value of the THz field was in its maximum $\max[E_{THz}(x, y, t)]$ was found. The vertical coordinates of the given maximum point was taken as $y = 0$. The zero horizontal coordinates as $x = 0$ when the system was put into the edge position. Fig. 4 and Fig. 5 show the time dependence of the THz electric field E_{THz} ($x = 1$ cm, $y = 0, t$) and $E_{THz}(x = 2$ cm, $y = 0, t)$, respectively. Fig. 6 depicts a two-dimensional spatial-time picture of the distribution of the amplitudes of THz field E_{THz} $(x, y = 0, t)$ using the spatial profile of the pump beam incident on the generating *InAs* crystal with $d = 2$ mm (Fig. 3a).

From Fig. 6, it can be seen that the wave front of THz radiation has a spatial-time anomaly. In the time plane E_{THz} ($x = 1.7$ cm, $y = 0, t$) there is a reduction of the field amplitude to zero. In addition, there is a transition point where the phase of the oscillation changes. For visual demonstration, Fig. 7 shows the normalized integrated intensity of THz radiation pattern of the coordinate x:

$$I_{THz}(x, y = 0) = \int |E_{THz}(x, y = 0, t)|^2 \, dt. \tag{1}$$

A similar spatial-temporal anomaly was observed in the case of the excitation by focused laser beam with diameter value of $d = 1$ mm (Fig. 8 on the right), and a beam of quasi-rectangular form (Fig. 8 on the left).

It should be noted that when decreasing the size of the excitation spot of THz radiation the wave front curvature is increased, and the area of maximum intensity of the THz field in the x axis decreases. When comparing the measured energy in a variety of fields of spots illuminating the crystal *InAs* it was found that the highest values of the electric field for THz radiation were achieved by focusing of the pump beam into a circular aperture with a diameter of 1 mm, which corresponds approximately to the maximum power density of the femtosecond

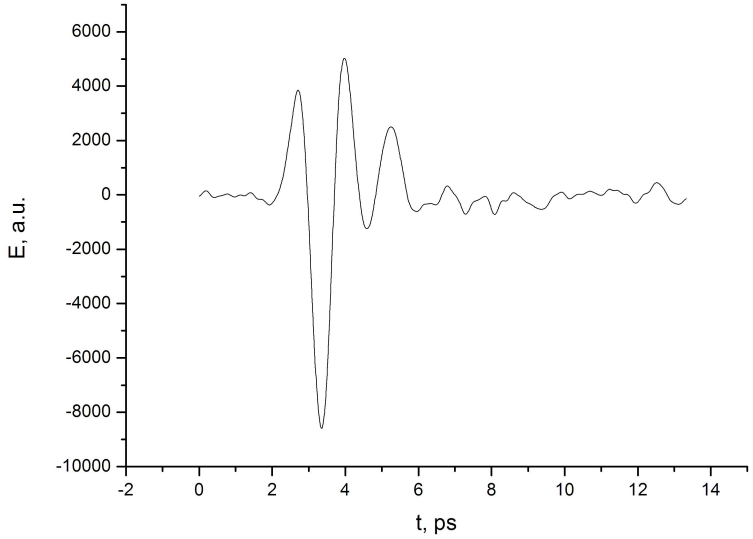

FIG. 4. Temporary form of the THz field in the focal plane of the spatial point E_{THz} ($x = 1$ cm, $y = 0, t$)

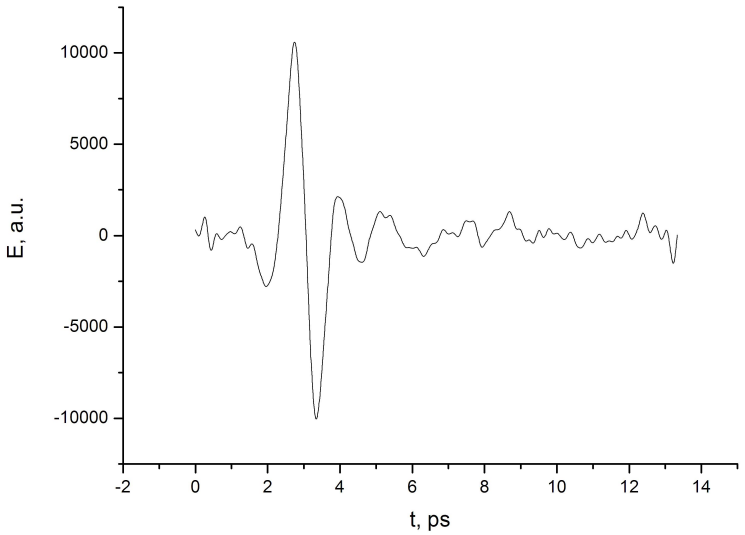

FIG. 5. Temporary form of the THz field in the focal plane of the spatial point E_{THz} ($x = 2$ cm, $y = 0, t$)

radiation. Thus, it is also the maximum efficiency of the energy transform from IR to the THz [2, 3].

The presence of the spatial-time anomaly in the diffraction pattern can be explained by the appearance of the phase shift larger than $\pi/2$ in the plane of the beam of THz radiation, which leads to an intensity dip in the far field [19]. A spatial phase shift can be caused by localized heating of the Teflon filter (P in Fig. 1), due to the powerful absorption of high intensity femtosecond laser beam. Additional studies are needed for explanation of this phenomenon.

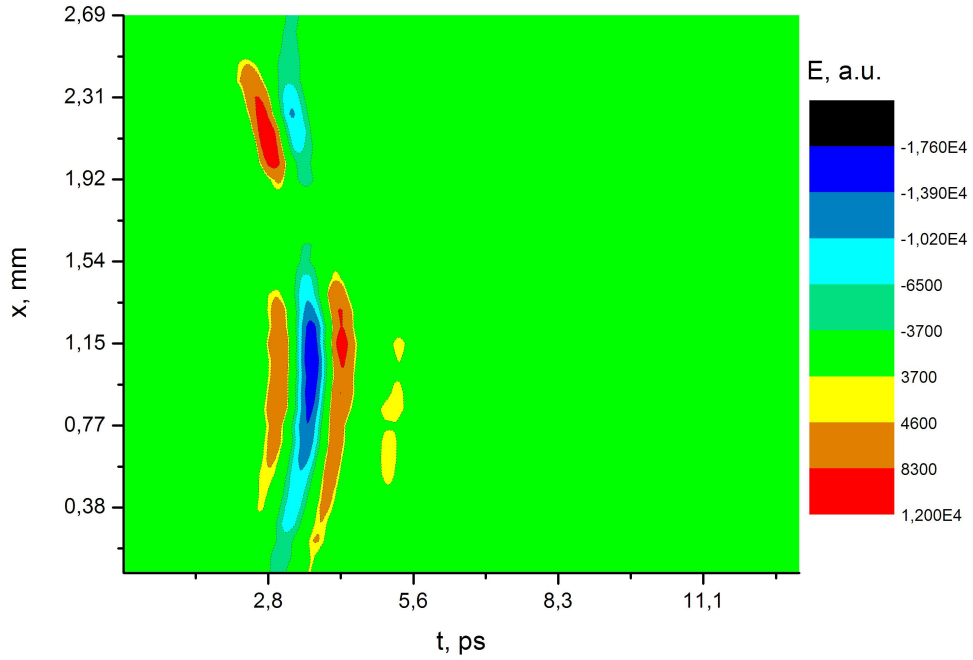

FIG. 6. Spatial-time picture of the amplitude distribution of THz field E_{THz} $(x, y = 0, t)$

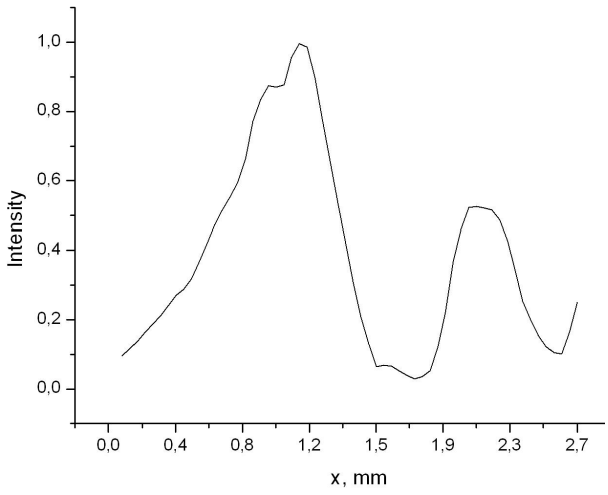

FIG. 7. Integrated picture of the intensity of THz radiation to the coordinate x I_{THz} $(x, y = 0)$

4. Conclusion

The scheme was proposed for an experimental setup, which was then assembled for measurements of the spatial and temporal patterns of the electric field amplitudes of THz radiation near a parabolic mirror focal plane. In these experiments different pump beam geometries of a femtosecond laser were used. Experimentally a spatial-time anomaly was observed in the diffraction patterns. In the wave front of the field the amplitude decreased to zero, and after going through this spatial plane, the phase of the oscillations changed. On the other hand, there was a dip in the integrated intensity curve. A spherical wave front in the observed diffraction patterns was observed, and by reducing the diameter of the excitation spot, the curvature of

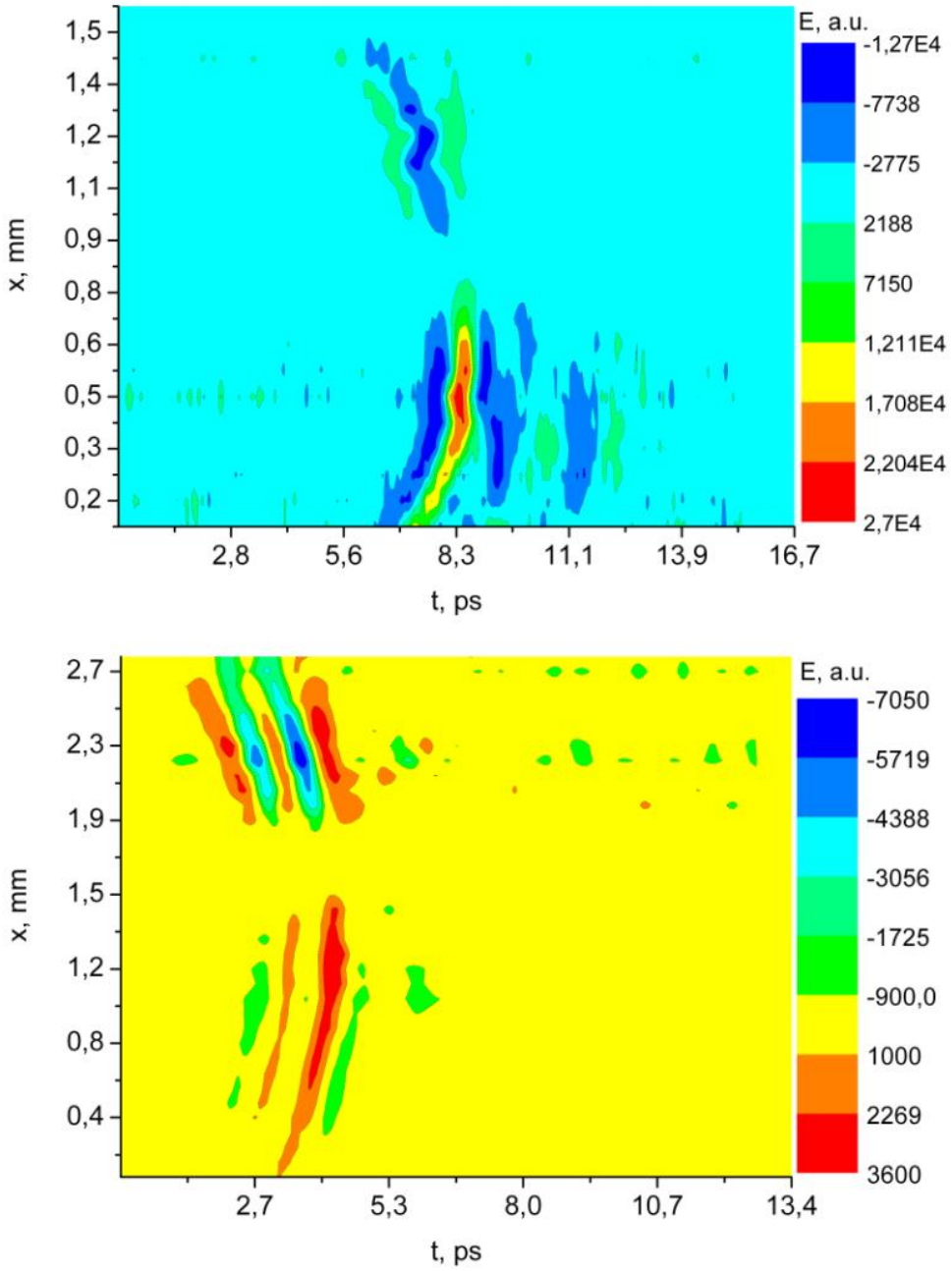

FIG. 8. Spatial-time picture of the amplitude distribution of THz field E_{THz} $(x, y = 0, t)$ in the case of the excitation laser focused beam with diameter $d = 1$ mm (right), and a beam of quasi-rectangular form 5×0.1 mm (left)

the THz wave front increased. So, the experiments show that the spatial non-uniformity of the THz field must be taken into consideration for correct spectroscopic measurements. It is also important to scan the THz pulse through the central peak of the diffraction pattern and the center of the sphere of the wave front, otherwise, the shape of the measured pulse will undergo a temporary distortion and the corresponding spectrum will be changed.

Acknowledgments

This work was supported by grant from the Ministry of Education and Science of the Russian Federation (projects No. 14.512.11.0020).

References

[1] A. Glagolewa-Arkadiewa. Short electromagnetic waves of wave-length up to 82 microns. *Nature*, **113** (2844), P. 640 (1924).
[2] X.C. Zhang, J. Xu. *Introduction to THz wave photonics*. NY., Springer, 246 pp. (2009).
[3] Y.-S. Lee. *Principles of terahertz science and technology*. Springer Science+Business Media, LLC, XII, 340 pp. (2009).
[4] B.B. Hu, X.C. Zhang, D.H. Auston. Terahertz Radiation Induced by Subbandgap Femtosecond Optical Excitation of gas. *Phys. Rev. Lett.*, **67**, P. 2709 (1991).
[5] V.G. Bespalov, V.N. Krylov, S.E. Putilin, D.I. Stasel'ko. Lasing in the far IR spectral range under femtosecond optical excitation of the inas semiconductor in a magnetic field. *Optics and Spectroscopy*, **93** (1), P. 148–152 (2002).
[6] Q. Wu, X.C. Zhang. Free-space electro-optic sampling of terahertz beams. *Appl. Phys. Lett.*, **67**, P. 3523 (1995).
[7] D.J. Cook, R.M. Hochstrasser. Intense terahertz pulses by four-wave rectification in air. *Optics Letters*, **25** (16), P. 1210–1212 (2000).
[8] V.G. Bespalov. Superbroad-band pulsed radiation in the terahertz region of the spectrum: production and application. *Journal of Optical Technology*, **73** (11), P. 764-771 (2006).
[9] N.N. Rozanov. On the diffraction of ultrashort pulses. *Optics and Spectroscopy*, **95** (2), P. 299–302 (2003).
[10] L. Sereda, A. Ferrari, M. Bertolotti. Spectral and time evolution in diffraction from a slit of polychromatic and nonstationary plane waves. *J. Opt. Soc. Am. B*, **13**, P. 1394–1402 (1996).
[11] X. Jingzhou, W. Li, Y. Guozhen. Effects of spectral linewidth of ultrashort pulses on the spatiotemporal distribution of diffraction fields. *Chinese Science Bulletin*, **46** (11), P. 901 (2001).
[12] A.A. Ezerskaya, D.V. Ivanov, V.G. Bespalov, S.A. Kozlov. Diffraction of single-period terahertz electromagnetic waves. *Journal of Optical Technology*, **78** (8), P. 551–557 (2011).
[13] C. Iaconis, I.A. Walmsley. Spectral phase Interferometry for direct electric-field reconstruction of ultrashort optical pulses. *Optics Letters*, **23**, P. 792–794 (1998).
[14] B.B. Hu, X.C. Zhang, D.H. Auston. Terahertz Radiation Induced by Subbandgap Femtosecond Optical Excitation of gaas. *Phys. Rev. Lett.*, **67**, P. 2709 (1991).
[15] N. Llombart, A. Neto. Thz Time-Domain Sensing: The Antenna Dispersion Problem and a Possible Solution. *Terahertz Science and Technology*, **2** (4), P. 416–423 (2012).
[16] D.T.F. Marple, H. Ehrenreich. Dielectric Constant Behavior Near Band Edges in CdTe and Ge. *Phys. Rev. Lett.*, **8**, P. 87–89 (1962).
[17] E.D. Palik, et al. *Handbook of Optical Constants of Solids*. Elsevier, 3227 pp. (1998).
[18] M.S. Kulya, Ya.V. Grachev, V.G. Bespalov. Obtaining topograms with use of pulsed terahertz reflectometr. *Nanosystems: Physics, Chemistry, Mathematics*, **3** (5), P. 33–41 (2012).
[19] J.W. Goodman. I*ntroduction To Fourier Optics*. McGraw-Hill, 441 pp. (1996).